# Crystal Engineering on Industrial Diaryl Pigments Using Lattice Energy Minimizations and X-ray Powder Diffraction

**Martin U. Schmidt,*,† Robert E. Dinnebier,‡ and Holger Kalkhof§**

*Institute for Inorganic and Analytical Chemistry, Johann Wolfgang Goethe-University, Max-von-Laue-Strasse 7, D-60438 Frankfurt am Main, Germany, Max-Planck-Institute for Solid State Research, Heisenbergstrasse 1, D-70569 Stuttgart, Germany, and Computational Chemistry, Jerini AG, Invalidenstrasse 130, D-10115 Berlin, Germany*

*Received: March 2, 2007*

Diaryl azo pigments play an important role as yellow pigments for printing inks, with an annual pigment production of more than 50,000 t. The crystal structures of Pigment Yellow 12 (PY12), Pigment Yellow 13 (PY13), Pigment Yellow 14 (PY14), and Pigment Yellow 83 (PY83) were determined from X-ray powder data using lattice energy minimizations and subsequent Rietveld refinements. Details of the lattice energy minimization procedure and of the development of a torsion potential for the biphenyl fragment are given. The Rietveld refinements were carried out using rigid bodies, or constraints. It was also possible to refine all atomic positions individually without any constraint or restraint, even for PY12 having 44 independent non-hydrogen atoms per asymmetric unit. For PY14 (23 independent non-hydrogen atoms), additionally all atomic isotropic temperature factors could be refined individually. PY12 crystallized in a herringbone arrangement with twisted biaryl fragments. PY13 and PY14 formed a layer structure of planar molecules. PY83 showed a herringbone structure with planar molecules. According to quantum mechanical calculations, the twisting of the biaryl fragment results in a lower color strength of the pigments, whereas changes in the substitution pattern have almost no influence on the color strength of a single molecule. Hence, the experimentally observed lower color strength of PY12 in comparison with that of PY13 and PY83 can be explained as a pure packing effect. Further lattice energy calculations explained that the four investigated pigments crystallize in three different structures because these structures are the energetically most favorable ones for each compound. For example, for PY13, PY14, or PY83, a PY12-analogous crystal structure would lead to considerably poorer lattice energies and lower densities. In contrast, lattice energy calculations revealed that PY12 could adopt a PY13-type structure with only slightly poorer energy. This structure was found experimentally as a metastable gamma phase of PY12. Calculations on mixed crystals (solid solutions) showed that mixed crystals of PY12 and PY13 should adopt the PY13 structure with planar molecules, resulting in high color strengths; this was proven experimentally (Pigment Yellow 188). Similarly, the high color strength of mixed crystals consisting of PY13 and PY14 (Pigment Yellow 174), and PY13/PY83 (Pigment Yellow 176) is explained by the crystal structures.

## 1. Introduction

Organic pigments are nowadays most commonly used for coloring paints and plastics and for most printing applications.[1] Diaryl pigments having the formula **1** are the most important ones used for yellow shades.

Annual production of diaryl pigments worldwide totals about 50 000 t, with a value of about $300 million. Pigment Yellow (PY) 12 has the highest production volume of any organic yellow pigment in the world. PY12 and PY13 are used for four-color printing; also, the cover for *The Journal of Physical Chemistry B* is printed using PY12.[2]

The industrial synthesis starts with a double diazotation of 3,3′-dichlorobenzidine, followed by coupling on the corresponding acetoacetylated anilines (Scheme 1). Synthesis is carried out in water, and the pigments precipitate as fine powders with particle sizes of less than 100 nm.

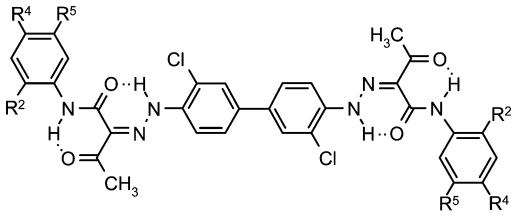

**1**

**a**: $R^2 = R^4 = R^5 = H$ (Pigment Yellow 12)

**b**: $R^2 = R^4 = CH_3$, $R^5 = H$ (Pigment Yellow 13)

**c**: $R^2 = CH_3$, $R^4 = R^5 = H$ (Pigment Yellow 14)

**d**: $R^2 = R^5 = O\text{-}CH_3$, $R^4 = Cl$ (Pigment Yellow 83)

Pigments are hardly soluble in the application medium (paint, printing ink, plastic, etc.). The pigment particles are simply finely dispersed. Therefore, the properties of the pigments (shade, tinctorial strength, light fastness, etc.) do not solely depend on the molecular structure but also on the particle size

* To whom correspondence should be addressed. E-mail: m.schmidt@chemie.uni-frankfurt.de. Fax: (+49) 69 798 29235.

† Johann Wolfgang Goethe-University.

‡ Max-Planck-Institute for Solid State Research.

§ Jerini AG.

10.1021/jp071731p CCC: $37.00 
Published on Web 08/02/2007

**SCHEME 1: Industrial Synthesis of Diaryl Pigments**

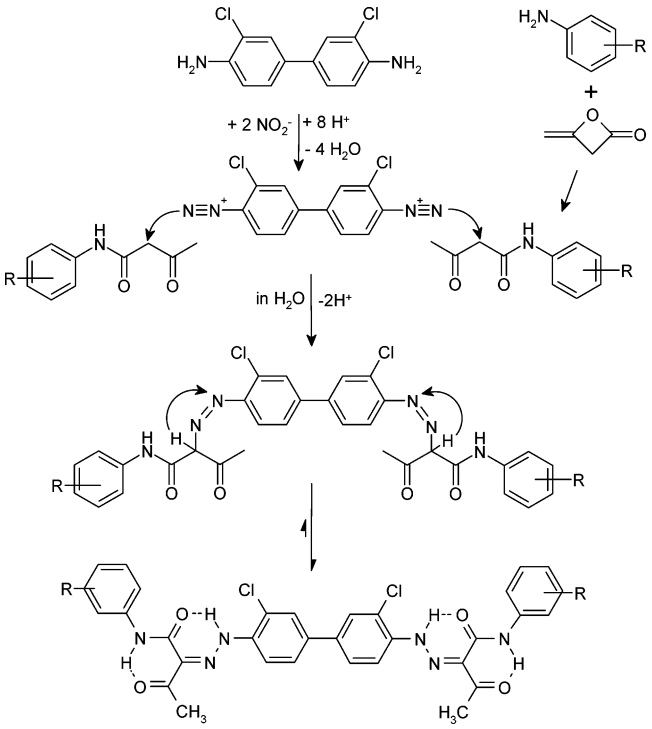

distribution and the crystal structure.[1] Knowledge of the crystal structures is essential for an understanding of structure−property relations, which are used to rationalize and specifically influence the properties of the pigments (crystal engineering). Therefore, efforts are being made globally to elucidate the crystal structures of all industrially produced pigments. All the more astounding is the fact that crystal structures of most diaryl pigments remained unknown for many years. Consequently, some properties were not understood either; for example, it was observed that the maximum achievable tinctorial strength of PY13 is about 50% higher than that for PY12. (i.e., to achieve a coloration of a desired shade, one needs 50% more pigment when PY12 is used instead of PY13).[3] In contrast, predictions with quantum mechanical calculations on individual molecules result in nearly identical tinctorial strengths regardless of the substitution pattern. Additional methyl groups have practically no influence on the $\pi$ system; PPP calculations on PY12, PY13, and PY14 with planar conformations give $f$ values of 2.74, 2.71, and 2.72, respectively. Hence, the increased tinctorial strength of PY13 with respect to PY12 seemed to be a solid-state phenomenon without it being possible to explain the reason.

Diaryl pigments are hardly soluble in all solvents, even at high temperature; hence, it is very difficult to grow single crystals for X-ray structure analysis. We therefore determined the crystal structures of PY12, PY13, PY14, and PY83 (**1a**−**d**) from X-ray powder diffraction data.

Crystal structure determination from powder data is much more challenging than from single-crystal data because, first, the information content of a powder diffractogram is markedly lower and, second, this information is considerably more difficult to extract because of the systematic and random overlapping of the diffraction reflections. Consequently, although about 300 000 single-crystal structure analyses of molecular compounds are cited in the literature, there are only a few hundred structures that have been solved from X-ray powder data without referring to an isotypic single-crystal structure.[4]

The general methodology for structure determinations from powder diffraction data consists of three steps, (1) indexing of the powder diagram, that is, determination of lattice parameters and space groups, (2) structure solution, that is, creation of a structure model as a starting point for Rietveld refinement, and (3) Rietveld refinement.[5,6]

For structure solution, three main alternative approaches are available: (1) determination of integrated reflection intensities and application of methods similar to those used for single-crystal X-ray analysis, for example, direct methods,[7−9] Patterson methods,[10,11] or maximum entropy methods. This approach requires diffraction data with high resolution and precision; (2) "real-space methods", that is, fit of calculated versus experimental powder diagrams by moving molecules or fragments inside the unit cell.[12−21] For this approach, the knowledge of (approximated) lattice parameters is required; (3) prediction of crystal structures by global optimization of the lattice energy.[22−24] In most cases, several structures are found within an energy range of a few kilojoules per mole above the global minimum. To find out which of the predicted crystal structures corresponds to the actual sample, powder diagrams of all low-energy structures are to be calculated and compared with experimental powder data. This approach works for unindexed, low-quality powder diagrams as well. Recently, the crystal structure of the violet pigment $C_{22}H_{12}Cl_2N_6O_4$ was solved from a nonindexed powder diagram with 12 broad diffraction peaks only.[25] Nevertheless, computing time can be reduced dramatically if the experimental lattice parameters can be used in the calculations.

We repeatedly used the third approach to successfully determine crystal structures of organic compounds from X-ray powder data.[26−29] Here, we used this method to determine the crystal structures of PY12, PY13, PY14, and PY83.

## 2. Experimental Section

The atomic coordinates of the refined crystal structures of PY12, PY13, PY14, and PY83 were deposited as supplementary publication no. CCDC-170802 to 170805 with the Cambridge Crystallographic Data Centre. Copies of the data can be obtained free of charge from the following address in the United Kingdom: CCDC, 12 Union Road, Cambridge CB21EZ. Fax: (+44)1223-336-033. E-mail: deposit@ccdc.cam.ac.uk. http://www.ccdc.cam.ac.uk/data_request/cif.

**2.1. Sample Preparation and X-ray Diffraction Experiments.** X-ray powder data from diaryl pigments directly taken from industrial production generally show very broad Bragg reflections caused by small particle sizes ($\leq$100 nm) and a high number of lattice defects (see Figure 1a). Most technical pigments also contain resins or other additives for reducing the crystal sizes, controlling the crystal morphologies, and improving the dispersibilities. Solving crystal structures from these low-quality powder diagrams is hardly possible. Hence, we synthesized the pure pigments in the laboratory and recrystallized them from boiling solvents. For PY12, PY13, and PY14, dichlorobenzene (bp 180 °C) was used; for PY83, we used nitrobenzene (bp 210 °C). In all cases, quite large quantities of solvents were necessary to dissolve the pigments completely. The solutions were cooled to room temperature within 2 days. Upon cooling, the material fell out as microcrystalline powders. We did not succeed in obtaining single crystals, but the particle size and crystal quality of the powders were improved substantially. This is reflected in powder diagrams of considerably better quality (see Figure 1b). The influence of the syntheses and aftertreatment on the quality of the powder diagrams was also nicely shown by Christie, Monteith, and Barrow.[30]

Laboratory X-ray powder diagrams were measured on a STOE-STADI-P diffractometer in Debye−Scherrer (transmis-

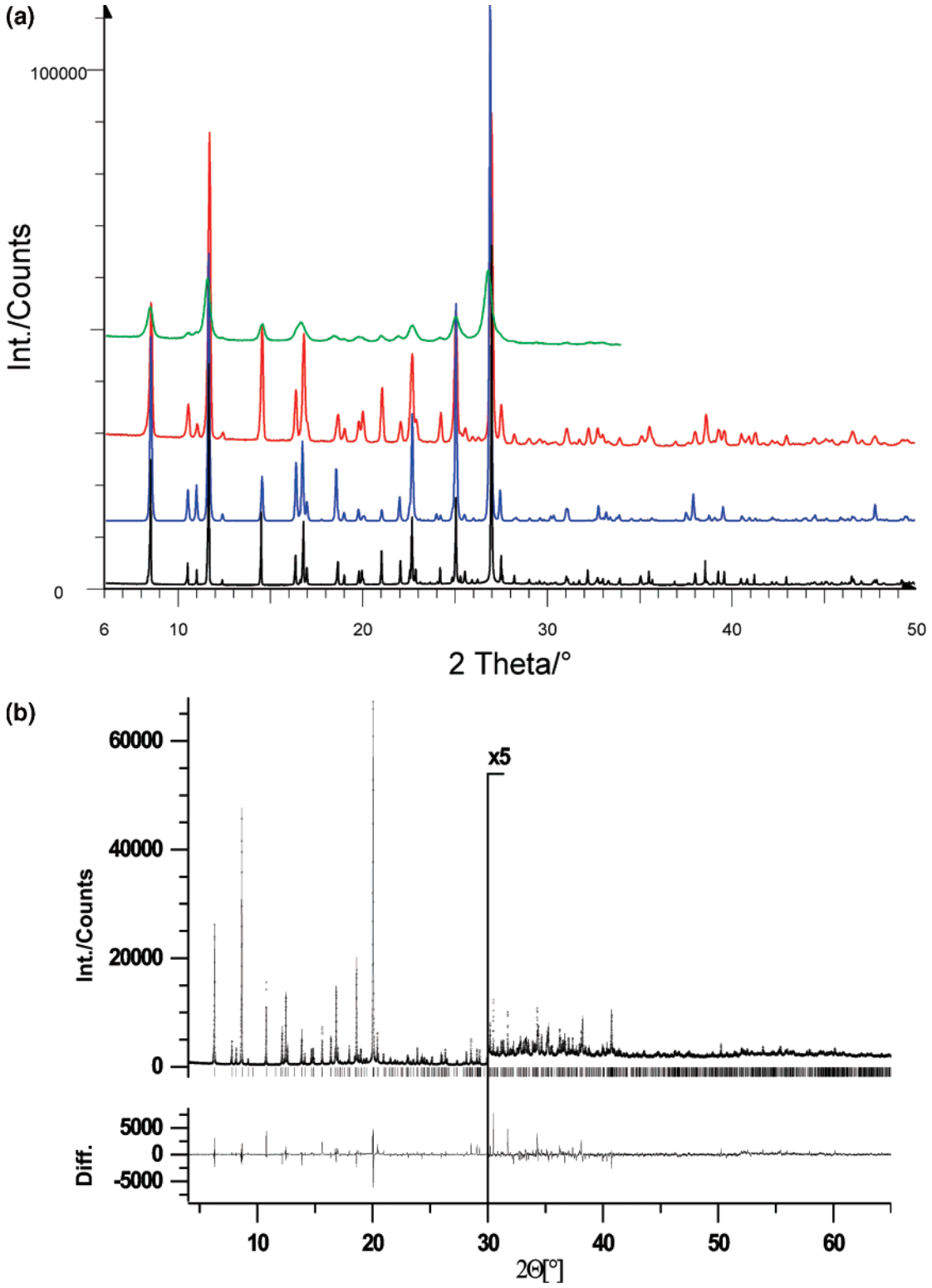


**Figure 1.** X-ray powder diagrams of PY14. (a) Top (green), sample from industrial production (laboratory data, $\lambda = 1.541$ Å); second (red), recrystallized product (laboratory data, $\lambda = 1.541$ Å); third (blue), simulated powder diagram of the calculated crystal structure having the lowest energy; bottom (black), recrystallized product (synchrotron data, $\lambda = 1.149$ Å, displayed in the scale of $\lambda = 1.541$ Å). (b) Rietveld plot; unconstrained Rietveld refinement of all nonhydrogen atoms using synchrotron data ($\lambda = 1.149$ Å): circles: experimental data; through line: calculated profile; bottom: difference curve.

sion) geometry. The diffractometer was equipped with a primary Ge(111) monochromator (Cu K$\alpha_1$ radiation, $\lambda = 1.54060$ Å) and a linear position-sensitive detector. Powder diagrams recorded in the range of $2\theta = 2-34°$, with a total measuring time of 2 h, turned out to be fully sufficient for indexing and crystal structure solution. For the Rietveld refinements, high-resolution powder diffraction data were collected at the SUNY X3B1 beamline at the National Synchrotron Light Source, Brookhaven National Laboratory, with the samples sealed in glass capillaries of 0.7 mm diameter for PY12, PY13, and PY83 and of 1.0 mm for PY14. X-rays of wavelengths 1.14818(2) Å for PY12, 1.14946(2) Å for PY13 and PY14, and 0.70002(2) Å for PY83 were selected by a double Si(111) monochromator. Wavelengths and the zero point have been determined from eight

well-defined reflections of the NBS1976 flat plate alumina standard. The diffracted beam was analyzed with a Ge(111) crystal and detected with a Na(Tl)I scintillation counter with a pulse height discriminator in the counting chain. The incoming beam was monitored by an ion chamber for normalization for the decay of the primary beam. In this parallel beam configuration, the resolution was determined by the analyzer crystal instead of by slits. Data were taken with the following parameters: PY12 (3.0−55.87° 2Θ; 0.005° 2Θ/step, 2.9 s/step); PY13 (5.0−42.19° 2Θ; 0.005° 2Θ/step, 3.3−5.3 s/step); PY14 (4.0−64.995° 2Θ; 0.005° 2Θ/step, 3.3−6.3 s/step); and PY83 (2.0−37.288° 2Θ; 0.004° 2Θ/step, 3.1−8.1 s/step). Although Θ scans did not show serious crystallite size effects, the samples were spun around Θ during measurement for better particle statistics. Low-angle diffraction peaks showed a strong asymmetry due to axial divergence and had a full-width at half-maximum (fwhm) of 0.01° 2Θ for PY83 and PY12, 0.022° 2Θ for PY13, and 0.017° 2Θ for PY14. Whereas the fwhm of the reflections of PY83 and PY12 was close to the resolution of the spectrometer, the reflections of PY13 and PY14 did show some sample-dependent isotropic peak broadening.

**2.2. Structure Solution by Lattice Energy Minimization.** *2.2.1. Molecular Geometry.* For global lattice energy optimizations, the knowledge of an (approximated) molecular geometry is required as input. Azo pigments can exist as azo or hydrazo tautomers (Scheme 1). Whereas in solution both tautomers are populated, in the solid state, all yellow azo pigments exist as the hydrazo tautomer because the acetoacetyl substituents form intramolecular hydrogen bonds between the acetyl and the hydrazo groups. This has been shown by single-crystal analyses of many mono-azo pigments of the Hansa Yellow type.[31,32] (Monoazo pigments are much more soluble than diazo pigments; therefore, single crystals of sufficient size and quality can be grown.)

The molecular geometry was derived from crystal structure data of similar molecules and fragments. A suitable model for PY12 would be the compound **2a** (reaction product of diazotized 2-chloro-aniline and *N*-acetoacetyl-aniline), which is a quasi-half of a molecule of PY12. Hence, we synthesized and crystallized the compound **2a** and determined the structure by single-crystal diffraction.[33] However, the structure of **2a** is effected by disorder. Therefore, we chose the crystal structure of **2b** (reaction product of diazotized aniline and *N*-acetoacetyl-2-methyl-aniline)[34] as a basis for the molecular geometry of **1a**−**d**, and only the geometry in the vicinity of the chlorine atom was taken from **2a**. For the central C−C bond, a length of 1.487 Å was assumed.[35] Additional substituents (methyl, chlorine, and methoxy) to the terminal phenyl fragments were added according to standard values[35] and data from the Cambridge Structural Database.[36] Furthermore, we assumed that overall molecular geometry is less influenced by the substituents.

Whereas the values of the bond length and bond angles could directly be transferred from the mono-azo pigments to PY12, PY13, PY14, and PY83, torsion angles are less rigid and can populate several minima. Furthermore, torsion angles for single bonds can be influenced by crystal packing forces. For example, unsubstituted biphenyl is known to be twisted by about 42° in the gas phase, but it is planar in the solid state. Consequently, we have to define 5 bonds as flexible in our simulations ($\vartheta_1$−$\vartheta_5$)

The values for the corresponding dihedral angles depend not only on the molecule itself but also on the crystal packing. If the molecules **1a**−**d** were situated on crystallographic inversion centers, then the following restraints were defined: $\vartheta_1 = 180°$,

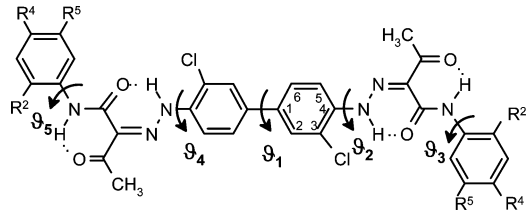


**1**

$\vartheta_2 = \vartheta_4$, $\vartheta_3 = \vartheta_5$; that is, an inversion center requires the biphenyl fragment to be planar. Since we did not know the conformation of the central biphenyl fragment, the rotational angle around the central single bond was refined together with the packing of the molecules. The same held for the torsion angles $\vartheta_2$−$\vartheta_5$. In the case of PY83, additionally, the four rotations around the Ph−$OCH_3$ bonds were refined.

*2.2.2. Development of Intramolecular Potentials.* Intramolecular potentials for the intramolecular degrees of freedom $\vartheta_1$−$\vartheta_5$ were derived from ab initio calculations as well as from statistical analyses of crystal structures from the Crystallographic Structural Database.

For the biphenyl torsion $\vartheta_1$, ab initio calculations on unsubstituted biphenyl were done on the MP2/DZP level using the program TURBOMOLE.[37] The calculated energies were multiplied by the factor 0.91 in order to adjust them to the barrier derived from a MP4(SDQ)/6-31G* calculation.[38] The resulting data points were fitted by a 6 term cosine series. To scale this potential with respect to the van der Waals energy, extensive global lattice energy minimizations on several biphenyl compounds have been performed.[39] The resulting potential is given by

$$E(\vartheta_1) = \sum_{n=0}^{6}(a_n \times \cos(n \times \vartheta_1)) \qquad (1)$$

with $a_0 = -19.34$, $a_1 = 6.84$, $a_2 = 10.01$, $a_3 = 1.99$, $a_4 = 0.36$, $a_5 = 0.11$, and $a_6 = 0.03$ kJ/mol.

Statistical analyses of crystal structures of substituted biphenyl compounds revealed that, in about half of the cases, the torsion angle $\vartheta_1$ is close to 0° (or 180°), whereas in the other cases, values around 30° (or 150°) are preferred. The occurrence of the 0° structures can be explained as a packing effect because planar molecules can generally be packed more densely.

For the rotation around the Ph−NN bond ($\vartheta_2$ and $\vartheta_4$), it is known from crystal structures of other azo pigments that the N−N moiety is almost coplanar with the benzene ring and always bent away from the chlorine atom, thus allowing a weak N−H···Cl hydrogen bond. For the torsion angles $\vartheta_2$ (C5−C4−N1−N2) and $\vartheta_4$ (C5′−C4′−N1′−N2′), a harmonic potential was used

$$E(\vartheta_{2,4}) = k(\vartheta_{2,4})^2 \qquad (2)$$

with $k = 0.1$ kJ/(mol·deg$^2$).

For the rotations $\vartheta_3$ and $\vartheta_5$, a search on the Cambridge Structural Database showed a broad distribution of torsion angles with a mean value of 0°; thus, we set up a harmonic potential (eq 2) with $k = 0.0025$ kJ/(mol·deg$^2$), which resulted in an energy of 1 kJ/mol at $\vartheta_3 = 20°$ and 4 kJ/mol at $\vartheta_3 = 40°$, the latter value being at the outer limit for typical torsion angles of the corresponding compounds.

*2.2.3. Intermolecular Energy.* The intermolecular energy was calculated by the atom−atom potential method.[40] The interatomic potential was set up as a sum of a van der Waals potential and a Coulomb term

$$E = \frac{1}{2}\sum_i \sum_j \left( -A_{ij} r_{ij}^{-6} + B_{ij} e^{-C_{ij} r_{ij}} + \frac{1}{4\pi\epsilon\epsilon_0} \frac{q_i q_j}{r_{ij}} \right) \quad (3)$$

where $r_{ij}$ is the interatomic distance between atoms $i$ and $j$, $A_{ij}$, $B_{ij}$, and $C_{ij}$ are the empirical van der Waals parameters for the interaction between atoms $i$ and $j$,[25,41] the $q$'s are the atomic charges, and $\epsilon$ is the relative dielectric constant, $\epsilon = 1$.

Atomic charges $q_i$ were calculated by the charge iteration EHT method with the ICON program.[42] The resulting charges, which are comparable to the Gasteiger[43] charges, were multiplied with an empirical factor of 1.1 to scale them with respect to the applied van der Waals potential. These charges have been proved to work well in combination with our van der Waals parameters.[44]

Hydrogen bond terms were not necessary in the description of the intermolecular energy since the pigments **1a**−**d** did not form intermolecular hydrogen bonds.

*2.2.4. Lattice Energy Minimizations.* The energy minimizations were performed with the CRYSCA[45,46] program, which carries out global optimization of the lattice energy. The minimizations started from a set of several thousand crystal structures with given lattice parameters and given possible space groups but random position and spatial orientation of the molecules. For the intramolecular degrees of freedom $\vartheta_1-\vartheta_5$, random start values within reasonable limits were similarly assumed. The energy was optimized by a special steepest descent method, varying the position and orientation of the molecules as well as the intramolecular torsion angles $\vartheta_1-\vartheta_5$. The lattice parameters were kept fixed. The obtained crystal structures were ranked according to energy and checked for higher symmetries.

**2.3. Rietveld Refinement.** The Rietveld refinements were carried out with the program package GSAS.[47] First of all, a LeBail fit[48] without structural model was performed to refine the lattice parameters and to optimize the peak shape parameters. The peak profile function was modeled using a multiterm Simpson's rule integration of the pseudo-Voigt function.[49] The strong asymmetry in the low angle region was described by a later implemented function,[50] which accounts for the asymmetry due to axial divergence. The background was manually determined with the program GUFI.[51] The resulting polygon was combined with a refinable 4 term cosine series. All profile and lattice parameters were fixed at the beginning of the Rietveld refinements.

By comparing the number of atoms (44−54 non-hydrogen per molecule) and the number of distinguishable peaks (110−225), it seemed quite unfavorable to refine all atomic coordinates individually. The number of possible degrees of freedom could therefore be dramatically reduced by the introduction of rigid bodies.[52] The effect was a strong increase of the ratio between linear independent observations and parameters, leading to a stabilized process of refinement. Furthermore, since the molecular fragments were forced to shift as a whole, meaningless changes could not occur.

In GSAS, a rigid body can be set up in various ways. The position of each atom within the rigid body is described as a combination of vectors given in Cartesian coordinates. The lengths of the vectors can be refined through a multiplier. For small molecules, the rigid body can be set up in a way that these vectors correspond to interatomic bonds, and thus, the position of an atom is the sum of several refinable interatomic vectors. For complex molecules like the diaryl pigments, this quickly becomes difficult to handle. A more comfortable way is to use the Cartesian coordinates of all atoms directly. Instead of refining individual bond lengths, an overall scale factor for the size of the molecule can be refined. The width and the height of the molecule can be refined individually by applying different multipliers to the three base vectors of the Cartesian coordinate system.

For the Rietveld refinements, the molecules of PY12−PY14 were divided in 3−6 rigid groups, which were held together by soft constraints, allowing constrained translations but individual rotations of the different groups. The number of refined parameters was increased step by step.

Because of the high quality of the powder pattern of PY83, the rigid bodies were replaced by soft constraints (44 for bond lengths, 55 for bond angles, and 7 for planarity), leading to an improved refinement.

As a final test for the correctness of the molecular geometry, all atomic positions were refined independently for three structures, after excluding the hydrogen atoms from the refinement. Although, the presumably flat molecular moieties like $C_6$ rings were slightly buckled, the positions of all non-hydrogen atoms remained close to their rigid-body positions, conforming the correctness of the molecular and structural model. Subsequent difference Fourier analysis revealed no considerable additional or missing electron density.

Drawings of the crystal structures were made with SCHAKAL.[53]

## 3. Results

**3.1. X-ray Diffraction and Energy Minimization.** The comparison of the X-ray powder diagrams of **1a**−**d** showed that only PY13 (**1b**) and PY14 (**1c**) are isotypic, whereas PY12 (**1a**) and PY83 (**1d**) have different crystal structures.

After recrystallizing the pigments, the laboratory powder diagrams of all pigments were indexed by TREOR[54] without ambiguity. The resulting lattice parameters are compiled in Table 1. The number of molecules per unit cell ($Z$) was determined by the rule "18 Å$^3$ per non-hydrogen atom".[55] Since pigments are known to pack more densely than general organic compounds, we used a value of 16 Å$^3$ instead of 18 Å$^3$. The resulting values for $Z$ are included in Table 1.

**TABLE 1: Lattice Parameters and Possible Crystal Symmetries from Indexing**

| compound | PY12 (**1a**) | PY13 (**1b**) | PY14 (**1c**) | PY83 (**1d**) |
|---|---|---|---|---|
| formula | $C_{32}H_{26}Cl_2N_6O_4$ | $C_{36}H_{34}Cl_2N_6O_4$ | $C_{34}H_{30}Cl_2N_6O_4$ | $C_{36}H_{32}Cl_4N_6O_8$ |
| $a$ (Å) | 17.867 | 8.369 | 8.209 | 5.190 |
| $b$ (Å) | 7.369 | 8.804 | 9.328 | 20.593 |
| $c$ (Å) | 24.060 | 12.478 | 11.773 | 16.982 |
| α (deg) | 90 | 71.29 | 112.59 | 90 |
| $\beta$ (deg) | 110.51 | 76.14 | 98.23 | 98.20 |
| $\gamma$ (deg) | 90 | 74.29 | 105.07 | 90 |
| $V$ (Å$^3$) | 2967.1 | 826.4 | 773.3 | 1796.5 |
| possible space groups | $P2_1/n$, ⋯ | $P1$, $P\bar{1}$ | $P1$, $P\bar{1}$ | $P2_1/c$, $Pc$, ⋯ |
| $Z$ | 4 | 1 | 1 | 2 |

For PY13 and PY14, the space group could either be $P1$ or $P\bar{1}$. If it was $P\bar{1}$, the molecule was situated on an inversion center. Since we did not know in advance if the molecule was planar and adopted inversion symmetry in the crystal, the energy minimizations had to be carried out without the inversion symmetry, that is, in space group $P1$. During the energy minimizations, in the lowest-energy packings and also many other packings, the molecules adopted conformations with inversion centers, that is, the resulting crystal structures could be described in space group $P\bar{1}$.

For PY12, the systematic extinctions led to the extinction symbol "$P - 2_1/n -$", corresponding to the space group $P2_1/n$.[56] The determination of systematic extinctions from powder diffraction data is, because of peak overlap, generally less reliable than that from single data. Thus, other space groups, ($P2_1$, $Pn$, $P2_1/m$, $P2/n$, $P2$, $Pm$, or $P2/m$) could not be excluded. All of these space groups are statistically less frequent than $P2_1/n$, especially for $Z = 4$;[57] therefore, the lattice energy minimization were started in $P2_1/n$, $Z = 4$, with one molecule per asymmetric unit, the molecule being located on a general position. The resulting low-energy packings did not show additional symmetries.

The systematic extinctions of PY83 led to the probable space groups $P2_1/c$ or $Pc$ (and some other, less frequently observed symmetries like $P2/c$). Lattice energy calculations were performed in $P2_1/c$, $Z = 2$, with molecules on inversion centers, and in $Pc$, $Z = 2$, with molecules on general positions. The low-energy structures of both calculations were identical, all exhibiting $P2_1/c$ symmetry with the molecule situated on a crystallographic inversion center.

For all predicted low-energy structures, X-ray powder diagrams were simulated. In all cases, packings with the best (lowest) energy gave simulated powder diagrams that were almost identical to the experimental powder diffractograms (see Figure 1c). Powder diagrams are very sensitive to small deviations in the crystal structures. The high similarity between calculated and experimental powder diagrams shows that the differences between the calculated and the actual crystal structures are on the order of 0.1 Å only.

We also investigated whether the crystal structures could also have been solved if the powder diagrams were not indexable. Therefore, calculations were carried out in the statistically most frequent space groups, with some thousand starting structures having random lattice parameters; the unit cells were optimized together with the position and orientation of the molecules and the intramolecular degrees of freedom. The calculation times were considerably higher than those for calculations with given unit cells. Nevertheless, for all four compounds, a minimum with good energy can be found, showing a simulated powder diagram similar to the experimental one. This minimum corresponds, in all cases, to the actual crystal structure. The accuracy of the crystal structures calculated without specification of the unit cell was, by far, sufficient for the Rietveld refinement. Hence, the crystal structures could also have been solved from nonindexable X-ray powder diagrams.

**3.2. Rietveld Refinements.** The calculated crystal structures were refined by the Rietveld method. Since we were interested in structural details such as torsion angles, high-resolution synchrotron powder diffractograms of all four compounds were recorded. The refined crystal structures were almost identical to the crystal structures calculated by energy minimization.

In order to prove that the molecules of PY13, PY14, and PY83 (**1b**−**d**) are planar, additional Rietveld refinements were carried out without the inversion centers, that is, in the corresponding subgroups. The refinements resulted in structures again showing inversion symmetries. Thus, the crystal symmetries found by lattice energy minimizations ($P2_1/n$, $P\bar{1}$, and $P2_1/c$) were confirmed by the Rietveld refinements.

The quality of the synchrotron powder data was so high that for PY12, PY13, and PY14 we tried for to refine all non-hydrogen atom positions individually without any constraints or restraints. To our astonishment, the refinements converged, even in the case of PY12 having 44 independent non-hydrogen atoms per asymmetric unit. This is, to our knowledge, one of the largest number of atoms in an unconstrained refinement hitherto. The atomic positions changed only slightly during refinement. In the case of PY14, it was even possible to refine all atomic isotropic temperature factors individually to reasonable values (Figure 1b, Table 2)!

A comparison of the molecular structures of PY12 obtained by rigid-body refinement and unconstrained refinement is given in Figure 2. The crystal structure of PY12 is shown in Figure 3.

After we had finished the structure determination of PY12,[58] Barrow et al.[59] reported that they succeeded in growing single crystals and determined the structure by single-crystal analysis. The single-crystal structure is very similar to our structure determined from X-ray powder data by rigid-body Rietveld refinement (see Figure 2). The average difference of the positions of non-hydrogen atoms is less than 0.1 Å. This shows the high accuracy of today's synchrotron powder diagrams. Also, the structures of PY13, PY14, and PY83[58,60−62] were well-confirmed by single-crystal structure determinations.[63,64]

**3.3. Characteristics of Crystal Structures and Structure−Property Relationships.** PY13 and PY14 are isostructural and form layer structures consisting of nearly planar molecules (Figures 4 and 5). In PY83, the molecules are planar as well but form a herringbone arrangement (Figure 6). PY12 crystallizes in a more complicated herringbone structure (Figure 3). In contrast to the other compounds, the molecules of PY12 are twisted around the central C−C bond by 21.7°. The two symmetrically independent halves of the molecule have different conformations; one is approximately planar, whereas in the other half, the terminal phenyl group is rotated by 28.7° (Figure 2). This twisting, especially of the biphenyl fragment, hinders the conjugation of the chromophoric $\pi$ systems and results in lower tinctorial strength, as also shown by PPP calculations.[65] Consequently, the smaller color strength of PY12 compared to that of PY13 is an effect of the molecular conformation caused by the crystal packing (Table 3).

**3.4. Why are the Structures Different?** Why do PY12, PY13, PY14, and PY83 crystallize with two different molecular conformations and in three different crystal structures, although the molecules differ only in the substitution pattern at the terminal phenyl rings? To answer this question, we calculated the lattice energies (including the intramolecular energies) by CRYSCA. Each compound was calculated in its own conformation and crystal structures, as well as in the (hypothetical) packings of the other pigments. In lattice energy minimizations, unit cell parameters were optimized simultaneously with the position and orientation of the molecules and the intramolecular degrees of freedom. This is necessary to be able to compare the energies of a molecules in different packing arrangements.

In the gas phase or in solution, all four compounds should adopt a twisted conformation of the biphenyl moiety since this is energetically more favorable than a planar conformation. In the crystal structures, this is realized for PY12 only. The planarity of PY13, PY14, and PY83 in the crystalline state is a

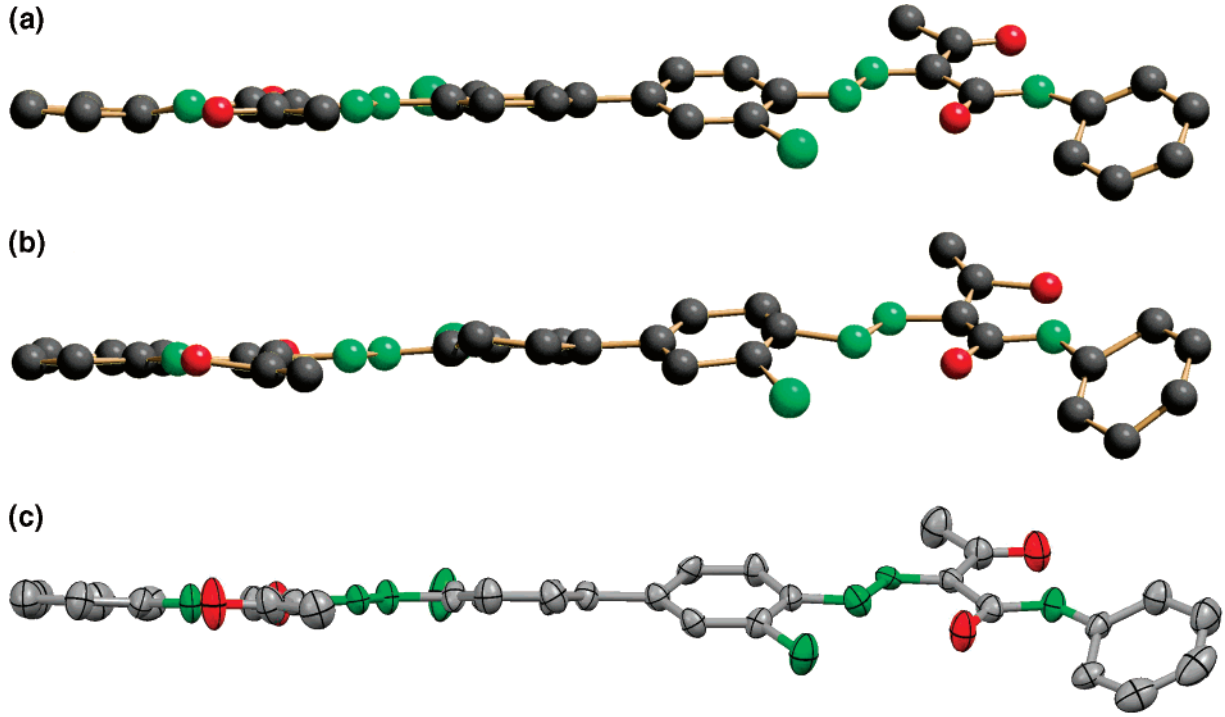


**Figure 2.** Comparison of different refinements for Pigment Yellow 12 (44 independent non-H atoms). (a) Synchrotron powder data; rigid-body Rietveld refinement. (b) Synchrotron powder data; unconstrained (!) Rietveld refinement of all non-hydrogen atoms. (c) Single-crystal data (Barrow et al., 2000), hydrogens omitted.

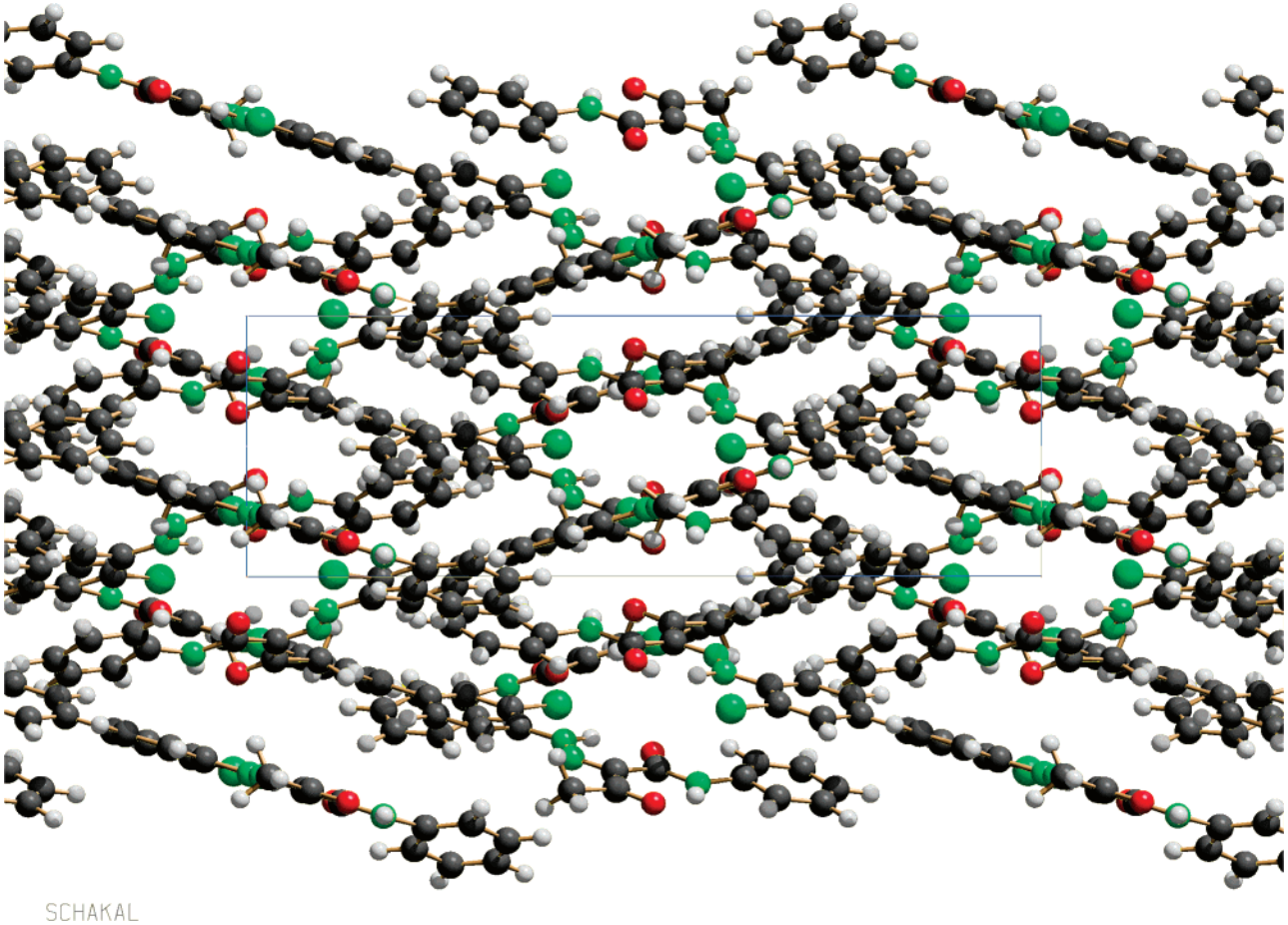


**Figure 3.** Crystal structure of PY12, (**1a**); view direction [1 0 0]

packing effect; the layer arrangement does not allow a substantial out-of-plane twisting of the molecules, and a PY12-analogous crystal structure would lead to markedly less favorable packings with lower densities and considerably poorer lattice energies owing to the steric requirements of the additional substituents. For PY12, PY13, and PY14, a PY83-type her-

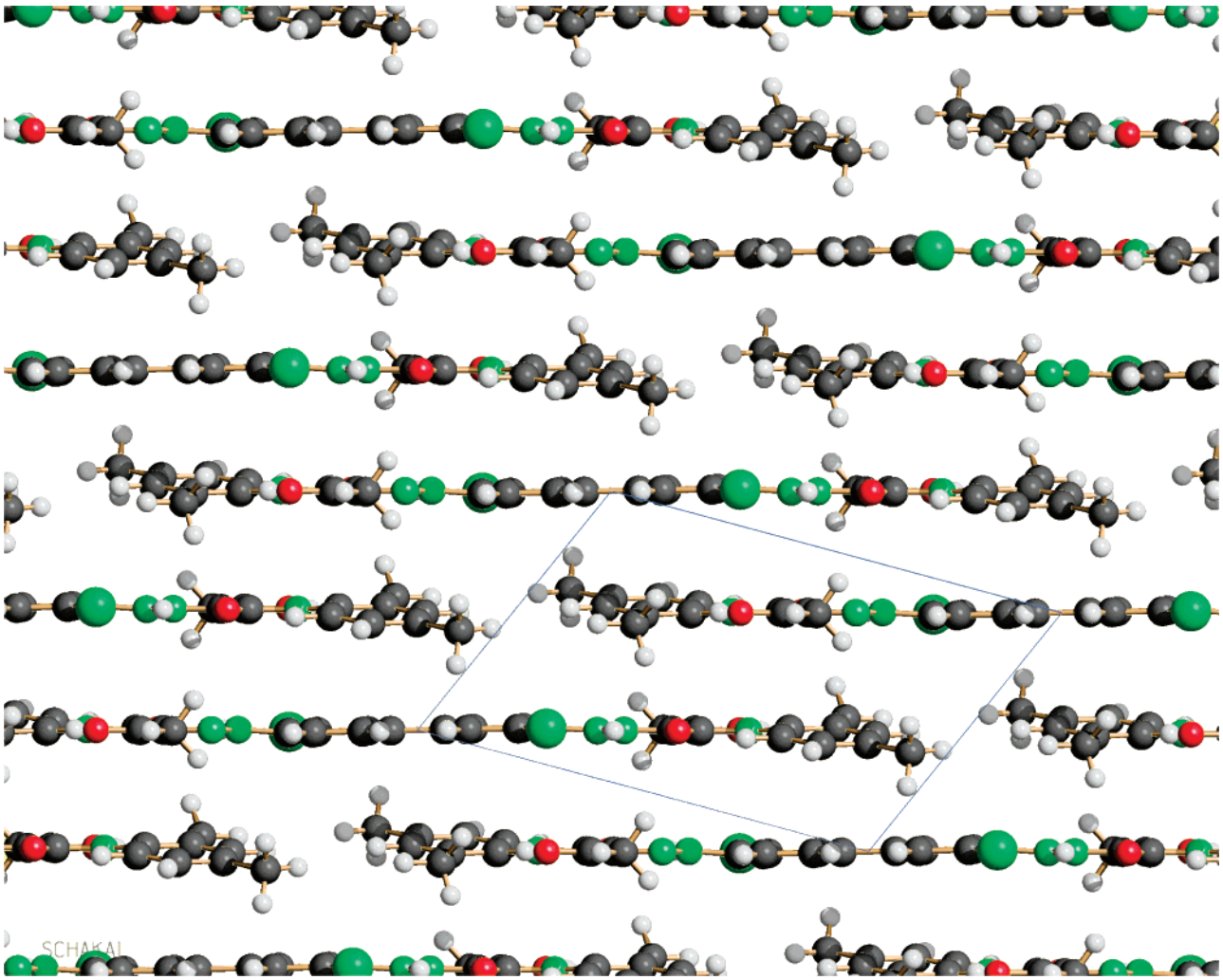

**Figure 4.** Crystal structure of PY13 (**1b**); view direction [1 0 0]. (PY14 (**1c**) is isostructural.)

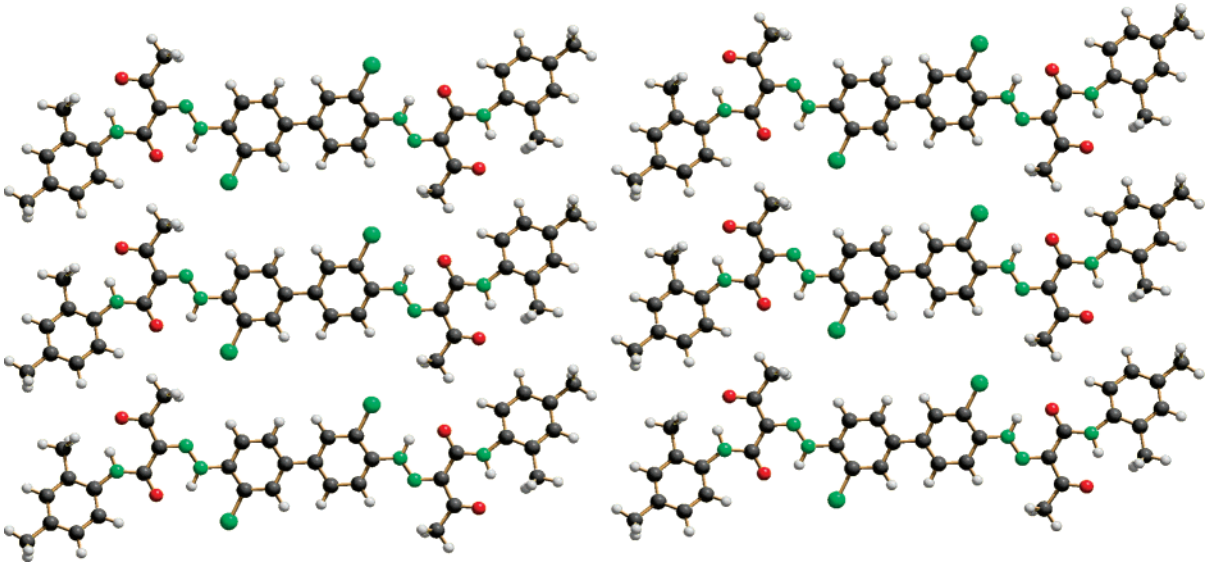

**Figure 5.** Crystal structure of PY13 (**1b**); view perpendicular to the molecular plane.

ringbone arrangement of planar molecules is unfavorable, both from the intramolecular and from the intermolecular energy aspect. Correspondingly, PY12- or PY83-type crystal structures have not yet been found for the other pigments experimentally (which does rule out the possibility that, one day, these metastable polymorphs may be found).

**3.5. Crystal Engineering.** Knowledge of the crystal structures can be used to improve physical properties of the pigments (crystal engineering). Our lattice energy calculations show that for PY12 the experimental herringbone arrangement has approximately the same intermolecular energy as a PY13-type layer arrangement of the molecules, that is, PY12 crystallizes

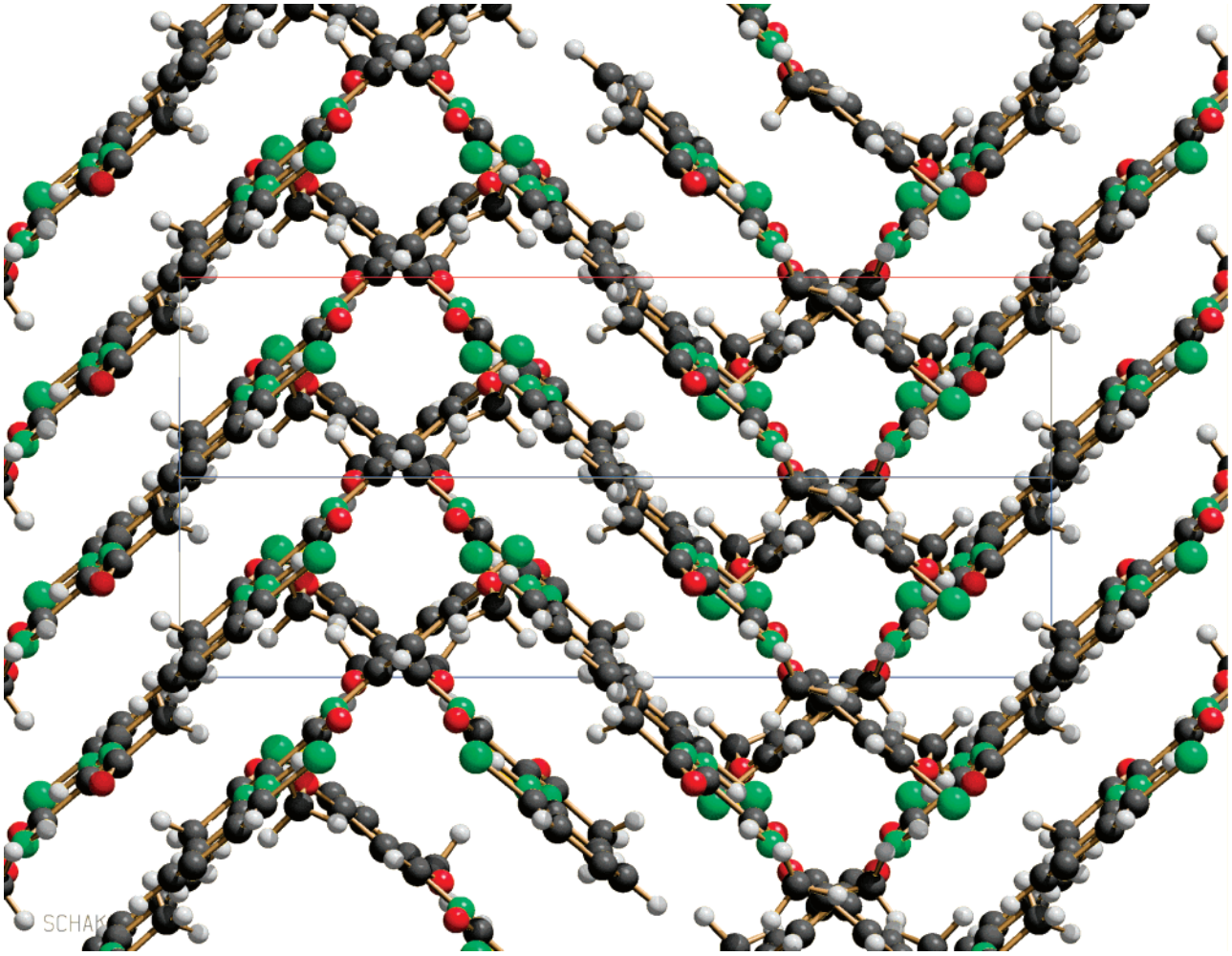

**Figure 6.** Crystal structure of PY83 (**1d**); view direction [1 0 $\bar{1}$].

in the herringbone arrangement because the molecule can assume the more favorable twisted conformation; a layer structure of planar molecules would be possible but would have worse total energy. This statement can be confirmed experimentally. There is a metastable polymorph[66] of PY12 which is isotypic to PY13 and PY14 (see Table 3). This $\gamma$-polymorph can be synthesized only with considerable amounts of special additives like dodecyldipropylenetriamine. (According to a patent,[67] there exists also a metastable $\beta$ phase of PY12, which is formed during some milling processes. We reproduced the described procedures, but we could not detect any trace of the $\beta$ phase. The powder diagram shown in the patent is of low quality and not suitable for solving the crystal structure; thus, the structure of $\beta$-PY12 remains unknown.)

Our crystal structure calculations show that molecules of different sizes can crystallize in the layer structure of PY13 and PY14 because the molecular layers can slide against each other relatively easily when the size of the molecules varies. Consequently, PY13 and PY14 form a continuous series of mixed crystals (solid solutions, single crystalline phase). This was proven in experiments.[68] As expected, the color strength of these mixed crystals is as high as that in PY13, regardless of the content of PY14. This mixed crystal is registered as PY174. Similarly, PY13 forms mixed crystals with Pigment Yellow 17 ($R^2 = O-CH_3$, $R^4 = H$), which are isostructural to PY13; these mixed crystals are registered as Pigment Yellow 127.

The synthesis of mixed crystals of diaryl pigments is quite easy since the mixed crystals are automatically formed if the synthesis is carried out with the mixture of the corresponding acetoacetylated anilines. Depending on the actual production process, the unsymmetrical compound is also formed (e.g., $R^4 = H$ on the left phenyl ring, but $R^4 = CH_3$ on the right ring). This unsymmetrical compound even facilitates the formation of solid solutions.

As predicted, mixtures of PY13 and PY83 also crystallize as solid solutions, forming the same layer structure as PY13 and PY14. This can be seen from the X-ray powder diagrams. As expected, these mixed crystals also show a high tinctorial strength (PY176; see Table 3).

According to the lattice energy calculations, also mixed crystals of PY14 and PY83, or PY14 and PY12, are predicted to crystallize in a PY13-like layer structure and exhibit high color strengths. For unknown reasons, these mixed crystals are not used industrially yet.

Most interesting are the mixtures of PY12 and PY13 that crystallize in the layer structure of PY13 too. In this crystal structure, PY12 has the planar conformation which has higher energy than the conformation in the herringbone arrangement of PY12. Nevertheless, these solid solutions are formed up to a content of 70% PY12. The solid solutions do not adopt a PY12-like structure since this would be energetically unfavorable because the additional methyl groups in PY13 do not fit into the herringbone packing of PY12. These mixed crystals have, in fact, been known and even produced industrially under the name PY188, and it was realized that they have high tinctorial strengths (like PY13), though the reason was not

**TABLE 2: Final Crystal Structures from Rietveld Refinement**

| | PY12 (**1a**) | PY13 (**1b**) | PY14 (**1c**) | PY83 (**1d**) |
|---|---|---|---|---|
| mol. formula | $C_{32}H_{26}Cl_2N_6O_4$ | $C_{36}H_{34}Cl_2N_6O_4$ | $C_{34}H_{30}Cl_2N_6O_4$ | $C_{36}H_{32}Cl_4N_6O_8$ |
| space group (no.) | $P2_1/c$ (No. 14) | $P\bar{1}$ (No. 2) | $P\bar{1}$ (No. 2) | $P2_1/n$ (No. 14) |
| Z | 4 | 1 | 1 | 2 |
| mol. site symmetry | 1 | $\bar{1}$ | $\bar{1}$ | $\bar{1}$ |
| $a$/Å | 17.878(4) | 8.3691(1) | 8.21420(6) | 5.18907(9) |
| $b$/Å | 7.365(2) | 8.7650(2) | 9.33011(5) | 20.6106(4) |
| $c$/Å | 24.365(5) | 12.8167(3) | 11.78471(8) | 16.9954(4) |
| $\alpha$/° | 90 | 112.054(1) | 112.6805(3) | 90 |
| $\beta$/° | 112.8(2) | 92.920(2) | 98.1609(4) | 98.186(1) |
| $\gamma$/° | 90 | 105.691(1) | 105.4338(4) | 90 |
| $V$/Å$^3$ | 2957(4) | 826.57(2) | 772.31(1) | 1799.13(6) |
| $\lambda$/Å | 1.148 | 1.149 | 1.149 | 0.700 |
| $2\theta$ range/° | 3−56 | 5−42 | 4−65 | 2−37.3 |
| no. of data points | 10574 | 7400 | 12200 | 8881 |
| no. of reflection positions | 1764 | 457 | 1379 | 1471 |
| no. of distinguishable peaks | 186 | 110 | 214 | 225 |
| | Constraint Rietveld Refinements | | | |
| refinement method | 4 rigid bodies | 3 rigid bodies | 3 rigid bodies | 132 constraints[a] |
| $R_p$, $R_{wp}$/% | 9.12, 12.69 | 7.06, 10.02 | 8.53, 12.87 | 7.38, 11.6 |
| $R_{F^2}$/% | 14.62 | 17.83 | 17.60 | 16.04 |
| $\chi^2$ | 3.8 | 3.1 | 3.3 | 2.63 |
| no. of variables | 21 | 11 | 15 | 139 |
| | Unconstraint Rietveld Refinements | | | |
| $R_p$, $R_{wp}$/% | 7.94, 10.63 | 6.25, 8.68 | 7.71, 11.09 | |
| $R_{F^2}$/% | 9.91 | 13.27 | 16.96 | |
| $\chi^2$ | 2.68 | 2.36 | 6.2 | |
| no. of variables | 134 | 74 | 99 | |

[a]Constraints: 44 bond lengths, 55 bond angles, 33 planar constraints.

**TABLE 3: Structure−Property Relationships in Diaryl Pigments**

| compound | achieved relative color strength[a] | molecular conformation | packing |
|---|---|---|---|
| PY12 | 100% | twisted | herring bone |
| PY12, $\gamma$ phase | n. n.[b] | planar | layer |
| PY13 | 141% | planar | layer |
| PY14 | (106%)[c] | planar | layer |
| PY83 | 138% | planar | herring bone |
| | Solid Solutions | | |
| PY188 (PY12 + PY13 + mixed compd.) | 150%[69] | planar | layer |
| PY174 (PY13 + PY14 + mixed compd.) | 151% | planar | layer |
| PY176 (PY13 + PY83 + mixed compd.) | 157% | planar | layer |

[a] The relative color strengths were calculated from the minimal amounts of pigments, which are necessary to achieve a coloration of 1/1 standard depth, according to the technical information on industrial pigments for printing inks.[3] The relative color strength of PY12 was set to 100%. [b] The $\gamma$ phase can be synthesized only with large amounts of special additives. [c] The technical product is not fully optimized. The maximum achievable color strength is estimated to be around 140%.[69]

known. Now, we can understand the high color strengths on the basis of the crystal structure of these solid solutions.

From the industrial point of view, mixed crystals of PY12 and PY13 have the advantage that they have similar physical properties as PY13 (i.e., high color strengths), but the production costs are lower because the starting materials of PY12 are cheaper than those for PY13 (because aniline is cheaper than 2,4-dimethylaniline. The production process itself is similar as that for pure PY13). This is a nice example of where crystal engineering helps to save millions of dollars per year.

## 4. Conclusions

Crystal structures of the diaryl pigments PY12, PY13, PY14, and PY83 were determined from X-ray powder diagrams by means of lattice energy minimizations and subsequent Rietveld refinements. The energy calculations also showed the reasons for the existence of three different crystal structures differing not only in their packing but also in molecular conformation. By combination of quantum mechanical calculations (for the individual molecules) and force-field calculations (for the lattice energy), we could explain the packings and their influence on the different coloristic properties of the pigments. Subsequently, crystal engineering was applied for the formation of mixed crystals having high color strengths.

The diaryl pigments are, at present, among the largest crystal structures solved by means of X-ray powder diffraction. However, neither energy minimization nor Rietveld refinement is restricted to molecules with 70−90 atoms. There are many compounds with 50−200 atoms (including active pharmaceutical ingredients), whose crystal structures arouse great interest but which cannot be solved by single-crystal X-ray structure analysis because single crystals cannot been grown. We are convinced that most of these crystal structures can be solved in the next few years from X-ray powder diagrams. As shown, the knowledge of the crystal structures can subsequently be used for crystal engineering, that is, for the targeted synthesis of compounds having improved solid-state properties.

**Acknowledgment.** The authors thank Professor Dr. Erich F. Paulus and Dipl-Ing. Ursula Conrad (both formerly at Hoechst AG, Frankfurt am Main) for the X-ray powder measurements, Professor Peter W. Stephens (SUNY at Stony Brook) for the synchrotron measurements, Dr. Heinz Schiffer (Hoechst AG, now at Clariant, Basel) for ab initio calculations, Professor Dr. Hans Jörg Lindner (Technical University of Darmstadt) for PPP calculations, and Dr. Hans Joachim Metz for ensuring excellent

working conditions at Clariant. The analyses of the yellow pigments used in the printed edition for the cover of *The Journal of Physical Chemistry B* were carried out by Fatima Cheurfa in the Clariant Analytical Services group (Frankfurt am Main). This project was financially supported by Clariant (Division Pigments & Additives, Pigments Research, Frankfurt), the Deutsche Forschungsgemeinschaft (German Research Society), and the U.S. Department of Energy, Division of Basic Energy Sciences (synchrotron measurements). This paper is dedicated to Professor Dr. Erich F. Paulus on the occasion of his 70th birthday.

## References and Notes

(1) Herbst, W.; Hunger, K. *Industrial Organic Pigments*, 3rd ed.; Wiley-VCH: Weinheim, Germany, 2004.

(2) Mass spectrometrical analysis of a small piece of the cover of the printed edition of *The Journal of Physical Chemistry B.*

(3) *Colorants for Printing Inks*; Technical information brochure, Clariant GmbH: Frankfurt am Main, 1999; update, 2000.

(4) Le Bail, A. Structure Determination from Powder Diffraction - Database. http://sdpd.univ-lemans.fr/iniref.html (2007).

(5) Rietveld, H. M. *Acta Crystallogr.* **1967**, *22*, 151.

(6) Rietveld, H. M. *J. Appl. Crystallogr.* **1969**, *2*, 65.

(7) Cascarano, G.; Favia, L.; Giacovazzo, C. *J. Appl. Crystallogr.* **1992**, *25*, 310.

(8) Altomare, A.; Burla, M. C.; Camalli, M.; Carrozzini, B.; Cascarano, G. L.; Giacovazzo, C.; Guagliardi, A.; Moliterni, A. C. G.; Polidori, G.; Rizzi, R. *J. Appl. Crystallogr.* **1999**, *32*, 339.

(9) Chan, F. C.; Anwar, J.; Cernik, R.; Barnes, P.; Wilson, R. M. *J. Appl. Crystallogr.* **1999**, *32*, 436.

(10) Wagner, K.; Hirschler, J.; Egert, E. *Z. Kristallogr.* **2001**, *216*, 565.

(11) Lasocha, W.; Czapkiewicz, J.; Milart, P.; Schenk, H. *Z. Kristallogr.* **2001**, *216*, 291.

(12) Harris, K. D. M.; Tremayne, M. *Chem. Mater.* **1996**, *8*, 2554.

(13) Harris, K. D. M.; Tremayne, M.; Kariuki, B. M. *Angew. Chem.* **2001**, *113*, 1674; *Angew. Chem., Int. Ed.* **2001**, *40*, 1626.

(14) Hammond, R. B.; Roberts, K. J.; Docherty, R.; Edmondson, M.; Gairns, R. *J. Chem. Soc., Perkin Trans. 2* **1996**, 1527.

(15) Tremayne, M.; Kariuki, B. M.; Harris, K. D. M. *J. Appl. Crystallogr.* **1996**, *29*, 211.

(16) Andreev, Yu. G.; Lightfoot, P.; Bruce, P. G. *J. Appl. Crystallogr.* **1997**, *30*, 294.

(17) Chernyshev, V. V.; Schenk, H. *Z. Kristallogr.* **1998**, *213*, 1.

(18) David, W. I. F.; Shankland, K.; Shankland, N. *Chem. Commun.* **1998**, 931.

(19) Engel, G. E.; Wilke, S.; König, O.; Harris, K. D. M.; Leusen, F. J. J. *J. Appl. Crystallgr.* **1999**, *32*, 1169.

(20) Kariuki, B. M.; Calcagno, P.; Harris, K. D. M.; Philp, D.; Johnston, R. L. *Angew. Chem.* **1999**, *111*, 860; *Angew. Chem., Int. Ed.* **1999**, *38*, 831.

(21) Dinnebier, R. E.; Sieger, P.; Nar, H.; Shankland, K.; David, W. I. F. *J. Pharm. Sci.* **2000**, *89*, 1465.

(22) Lommerse, J. P. M.; Motherwell, W. D. S.; Ammon, H. L.; Dunitz, J. D.; Gavezzotti, A.; Hofmann, D. W. M.; Leusen, F. J. J.; Mooij, W. T. M.; Price, S. L.; Schweizer, B.; Schmidt, M. U.; van Eijck, B. P.; Verwer, P.; Williams, D. E. *Acta Crystallogr., Sect. B* **2000**, *56*, 697.

(23) Motherwell, W. D. S.; Ammon, H. L.; Dunitz, J. D.; Dzyabchenko, A.; Erk, P.; Gavezzotti, A.; Hofmann, D. W. M.; Leusen, F. J. J.; Lommerse, J. P. M.; Mooij, W. T. M.; Price, S. L.; Scheraga, H.; Schweizer, B.; Schmidt, M. U.; van Eijck, B. P.; Verwer, P.; Williams, D. E. *Acta Crystallogr., Sect. B* **2002**, *58*, 647.

(24) Day, G. M.; Motherwell, W. D. S.; Ammon, H. L.; Boerrigter, S. X. M.; Della Valle, R. G.; Venuti, E.; Dzyabchenko, A.; Dunitz, J. D.; Schweizer, B.; van Eijck, B. P.; Erk, P.; Facelli, J. C.; Bazterra, V. E.; Ferraro, M. B.; Hofmann, D. W. M.; Leusen, F. J. J.; Liang, C.; Pantelides, C. C.; Karamertzanis, P. G.; Price, S. L.; Lewis, T. C.; Nowell, H.; Torrisi, A.; Scheraga, H. A.; Arnautova, Y. A.; Schmidt, M. U.; Verwer, P. *Acta Crystallogr., Sect. B* **2005**, *61*, 511.

(25) Schmidt, M. U.; Ermrich, M.; Dinnebier, R. E. *Acta Crystallogr., Sect. B* **2005**, *61*, 37.

(26) Schmidt, M. U.; Dinnebier, R. E. *J. Appl. Crystallogr.* **1999**, *32*, 178.

(27) Schmidt, M. U. In *Crystal Engineering: From Molecules and Crystals to Materials*; Braga, D., Grepioni, F., Orpen, A. G., Eds. Kluwer Academic Publishers: Dordrecht, The Netherlands, 1999; pp 331−348.

(28) Schmidt, M. U.; Ermrich, M.; Dinnebier, R. E. *Acta Crystallogr. Sect. B* **2005**, *61*, 37.

(29) Schmidt, M. U.; Hofmann, D. W. M.; Buchsbaum, C.; Metz, H. J. *Angew. Chem.* **2006**, *118*, 1335; Schmidt, M. U.; Hofmann, D. W. M.; Buchsbaum, C.; Metz, H. J. *Angew. Chem., Int. Ed.* **2006**, *45*, 1313.

(30) Christie, R. M.; Monteith, J. E.; Barrow, M. J. *Surf. Coat. Int., Part B* **2003**, *86*, 247.

(31) Paulus, E. F. *Z. Kristallogr.* **1983**, *165*, 137.

(32) Whitaker, A. *Acta Crystallogr., Sect. C* **1987**, *43*, 2141.

(33) Paulus, E. F. Unpublished results.

(34) Paulus, E. F.; Rieper, W. *Acta Crystallogr., Sect. A* **1984**, *40*, C277.

(35) Allen, F. H.; Kennard, O.; Watson, D. G.; Brammer, L.; Orpen, A. G.; Taylor, R. *J. Chem. Soc., Perkin Trans.* **1987**, *2*, S1.

(36) *Cambridge Structural Database*; Cambridge Crystallographic Data Centre: 12 Union Road, Cambridge, England.

(37) Ahlrichs, R.; von Arnim, M. *Methods and Techniques in Computational Chemistry METECC-95*; STEF: Cagliari, 1995, pp 509−554.

(38) Tsusuki, S.; Tanabe, K. *J. Phys. Chem.* **1991**, *95*, 139.

(39) Kalkhof, H. Dissertation, Technical University, Darmstadt, Germany, 2002.

(40) Pertsin, A. J.; Kitajgorodsky, A. I. *The Atom-Atom Potential Method*; Springer-Verlag: New York, 1987.

(41) Schmidt, M. U. In *Crystal Engineering: From Molecules and Crystals to Materials*; Braga, D., Orpen, G.; Kluwer Academic Publishers: Dordrecht, The Netherlands, 1999, pp 331−348.

(42) Howell, J.; Rossi, A.; Wallace, D.; Haraki, K.; Hoffmann, R. *Quantum Chemical Programs Exchange* **1977**, *11*, 344; QCPE No. 517.

(43) Gasteiger, J.; Marsili, M. *Tetrahedron* **1980**, *36*, 3219.

(44) Schmidt, M. U. *Kristallstrukturberechnungen Metallorganischer Molekülverbindungen*; Verlag Shaker: Aachen, Germany, 1995.

(45) Schmidt, M. U.; Kalkhof, H. *CRYSCA, Program for crystal structure calculations of flexible molecules*; Frankfurt am Main, 1997.

(46) Schmidt, M. U.; Englert, U. *J. Chem. Soc., Dalton Trans.* **1996**, 2077.

(47) Larson, C.; von Dreele R. B. *Los Alamos National Laboratory Report*; LAUR 86−748, GSAS 1994, version 2002 V, 2002.

(48) Le Bail, A.; Duroy, H.; Fourquet, J. L. *Mater. Res. Bull.* **1988**, *23*, 447.

(49) Thompson, P.; Cox, D. E.; Hastings, J. B. *J. Appl. Crystallogr.* **1987**, *20*, 79.

(50) Finger, L. W.; Cox, D. E.; Jephcoat, A. P. *J. Appl. Crystallogr.* **1994**, *27*, 892.

(51) Dinnebier, R. E.; Finger, L. *Z. Kristallogr. Suppl.* **1998**, *15*, 148.

(52) Dinnebier, R. E. *Powder Diffr.* **1999**, *14*, 84.

(53) Keller, E. *SCHAKAL99*. Kristallographisches Institut der Universität: Freiburg, 1999.

(54) Werner, P.-E. *Z. Kristallogr.* **1964**, *120*, 375.

(55) Kempster, C. J. E.; Lipson, H. *Acta Crystallogr., Sect. B* **1972**, *28*, 3764.

(56) *International Tables for Crystallography, Volume A: Space group symmetry*, 5th ed.; Hahn, T., Ed.; Kluwer Academic Publishers: Dordrecht, The Netherlands, 2000.

(57) Belsky, V. K.; Zorkaya, O. N.; Zorky, P. M. *Acta Crystallogr., Sect. A* **1995**, *51*, 473.

(58) Schmidt, M. U. In *Colour Science '98, Vol. 1: Dye and Pigment Chemistry*; Griffiths, J. Ed.; University of Leeds: Leeds, U.K. 1999, pp 72−81; ISBN 0-85316-196-8.

(59) Barrow, M. J.; Christie, R. M.; Lough, A. J.; Monteith, J. E.; Standring, P. N. *Dyes Pigm.* **2000**, *45*, 153.

(60) Schmidt, M. U.; Dinnebier, R. E.; Kalkhof, H. *Z. Kristallogr. Suppl.* **1998**, *15*, 72.

(61) Schmidt, M. U.; Dinnebier, R. E. Presentation at the IUCr-XVIII Conference, Glasgow, U.K., August 4−13, 1999.

(62) Schmidt, M. U.; Dinnebier, R. E.; Kalkhof, H. Presentation at the 19th European Crystallographic Meeting, Nancy, France, August 26−31, 2000; p 129.

(63) Barrow, M. J.; Christie, R. M.; Monteith, J. E. *Dyes Pigm.* **2002**, *55*, 79.

(64) Barrow, M. J.; Christie, R. M.; Badcock, T. D. *Dyes Pigm.* **2003**, *57*, 99.

(65) Christie, R. M.; Standring, P. N. *Dyes Pigm.* **1989**, *11*, 109.

(66) Tuck, B.; Stirling, J. A.; Farnocchi, C. J.; McKay, R. B. (Ciba SC), European Patent EP 0790282 A2, 1997.

(67) Kawamura, T. Japanese Patent JP 62153353, 1987.

(68) Tanaka, K.; Takagi, K.; Haginoya, M.; Nakazima, E. *Shikizai Kyokaishi* **1963**, *36*, 392.

(69) Ott, U. (Clariant), personal communication.